Journal of Materials Chemistry C

Aggregation-Induced Emission Enhancement in Boron Difluoride Complexes of 3-Cyanoformazanates

Journal:	*Journal of Materials Chemistry C*
Manuscript ID	TC-COM-05-2016-001782.R1
Article Type:	Communication
Date Submitted by the Author:	12-Jun-2016
Complete List of Authors:	Maar, Ryan; The University of Western Ontario, Department of Chemistry Gilroy, Joe; The University of Western Ontario, Department of Chemistry

Journal of Materials Chemistry C

COMMUNICATION

Aggregation-Induced Emission Enhancement in Boron Difluoride Complexes of 3-Cyanoformazanates

Received 00th January 20xx,
Accepted 00th January 20xx

DOI: 10.1039/x0xx00000x

www.rsc.org/

Ryan R. Maar[a] and Joe B. Gilroy[a]*

Boron difluoride (BF_2) complexes of 3-cyanoformazanates exhibit aggregation-induced emission enhancement in THF-water mixtures due to their severely twisted *N*-aryl substituents which restrict intramolecular motion and π stacking upon aggregation.

Molecules that exhibit aggregation-induced emission (AIE) or aggregation-induced emission enhancement (AIEE) have garnered significant attention due to their applicability to the fields of organic electronics,[1,2] chemical sensing,[3,4] and fluorescence cell imaging.[1b, 5,6] Typically, organic fluorophores experience attenuated emission intensity upon aggregation as a result of aggregation-caused quenching (ACQ).[7] This arises due to the formation of strong intermolecular π-π stacking interactions enabling the formation of excimers/exciplexes, which quench excited states via non-radiative pathways.[1b]

The phenomenon of AIE was first described by Tang and co-workers as part of their work on 1-methyl-1,2,3,4,5-pentaphenylsilole **1**.[8] Since its discovery, significant efforts have been invested toward the elucidation of the mechanism of AIE. Ultimately, it has been proposed that the restriction of intramolecular motions (RIM), which includes the restriction of intramolecular rotations and restriction of intramolecular vibrations, leads to the AIE phenomenon.[5] Fervent work done by researchers worldwide has led to the development of numerous AIE luminogens (AIEgens), including: hydrocarbon-,[9] heteroatom-,[10] and boron-containing systems.[11,12] More recently, a variety of substituted tetraphenylethylenes **2**[13,14] and triphenylamines **3**[15] have been widely studied.

Boron difluoride (BF_2) formazanates are an interesting class of molecular materials that possess tunable absorption, emission, and electrochemical properties through structural variation.[16] The parent formazans **4**,[17] are commonly used in cell viability assays,[18] and are generally prepared via straightforward aryl diazonium coupling reactions in aqueous media. BF_2 formazanates have been incorporated into polymers,[19] explored as electrochemiluminescent materials,[20] used as precursors to B(I) carbenoid intermediates,[21] and employed as fluorescent cell-imaging agents.[22] Herein, we report the first examples of BF_2 formazanates that demonstrate AIEE.

BF_2 complex **5c** was prepared in 96% yield according to a well-established synthetic methodology and the synthesis and characterization of **5a** and **5b** have been reported elsewhere.[16, 22] We chose these methoxy-substituted compounds for this study due to their superior emission properties, specifically, their relatively higher fluorescence quantum yields (Φ_F) relative to other substituted BF_2 formazanate derivatives.[22] Complex **5c** was fully characterized using multinuclear NMR spectroscopy, UV-vis absorption and emission spectroscopy, IR spectroscopy, cyclic voltammetry, and high-resolution mass spectrometry (Figs. S1−S4).

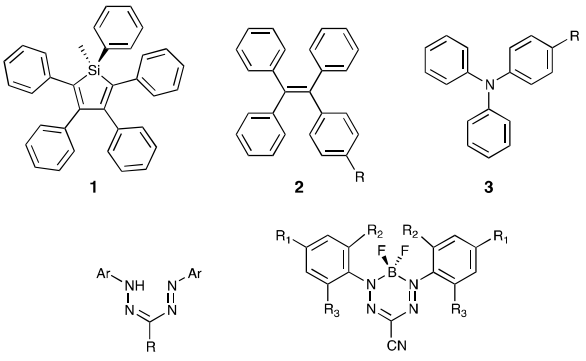

1 2 3 4

5a: R_1 = OMe, R_2 = R_3 = H
5b: R_1 = H, R_2 = OMe, R_3 = H
5c: R_1 = H, R_2 = R_3 = OMe

[a]*Department of Chemistry and the Centre for Advanced Materials and Biomaterials Research (CAMBR), The University of Western Ontario, London, Ontario, N6A 5B7 (Canada). *E-mail: joe.gilroy@uwo.ca*

†Electronic supplementary information (ESI) available: Synthesis and characterization details. CCDC 1455864. For ESI and crystallographic data in CIF or other electronic format see DOI: 10.1039/x0xx00000x

Compounds **5a–c** absorb and emit within the visible region of the electromagnetic spectrum with a noticeable blue-shift in the wavelength of maximum absorbance (λ_{abs}) when the *N*-aryl substituents were varied from 4-methoxyphenyl (**5a**: λ_{abs} = 556 nm; ε = 33,400 M^{-1} cm^{-1}) to 2-methoxyphenyl (**5b**: λ_{abs} = 456 nm; ε = 10,100 M^{-1} cm^{-1}) to 2,6-dimethoxyphenyl (**5c**: λ_{abs} = 434 nm; ε = 13,900 M^{-1} cm^{-1}) (Fig. 1 and Table S1). This trend was also evident when examining the wavelength of maximum emission (λ_{em}) for **5a** (λ_{em} = 662 nm), **5b** (λ_{em} = 590 nm), and **5c** (λ_{em} = 556 nm). The trends observed for the absorption/emission maxima are consistent with a previous report where the presence of *ortho* substituents led to twisting of the *N*-aryl substituents relative to the formazanate backbone and a blue-shift in absorption/emission maxima.[22] A decrease in the Φ_F was also observed for the same series of compounds: **5a** (Φ_F = 0.46), **5b** (Φ_F = 0.03) and **5c** (Φ_F < 0.01) (Figs. S5, S6, and Table S1).[23] The solid-state structures of **5a–c** are comprised of carbon-nitrogen and nitrogen-nitrogen bonds with lengths between those of typical single and double bonds of the respective atoms, indicating a delocalized formazanate backbone consistent with previous reports (Tables S2 and S3).[22] In addition, the dihedral angles between the *N*-aryl substituents and the formazanate backbone deviate from planarity from 4-methoxyphenyl (**5a**: 15.3°, 21.4°; 47.7°, 47.7°)[‡] to 2-

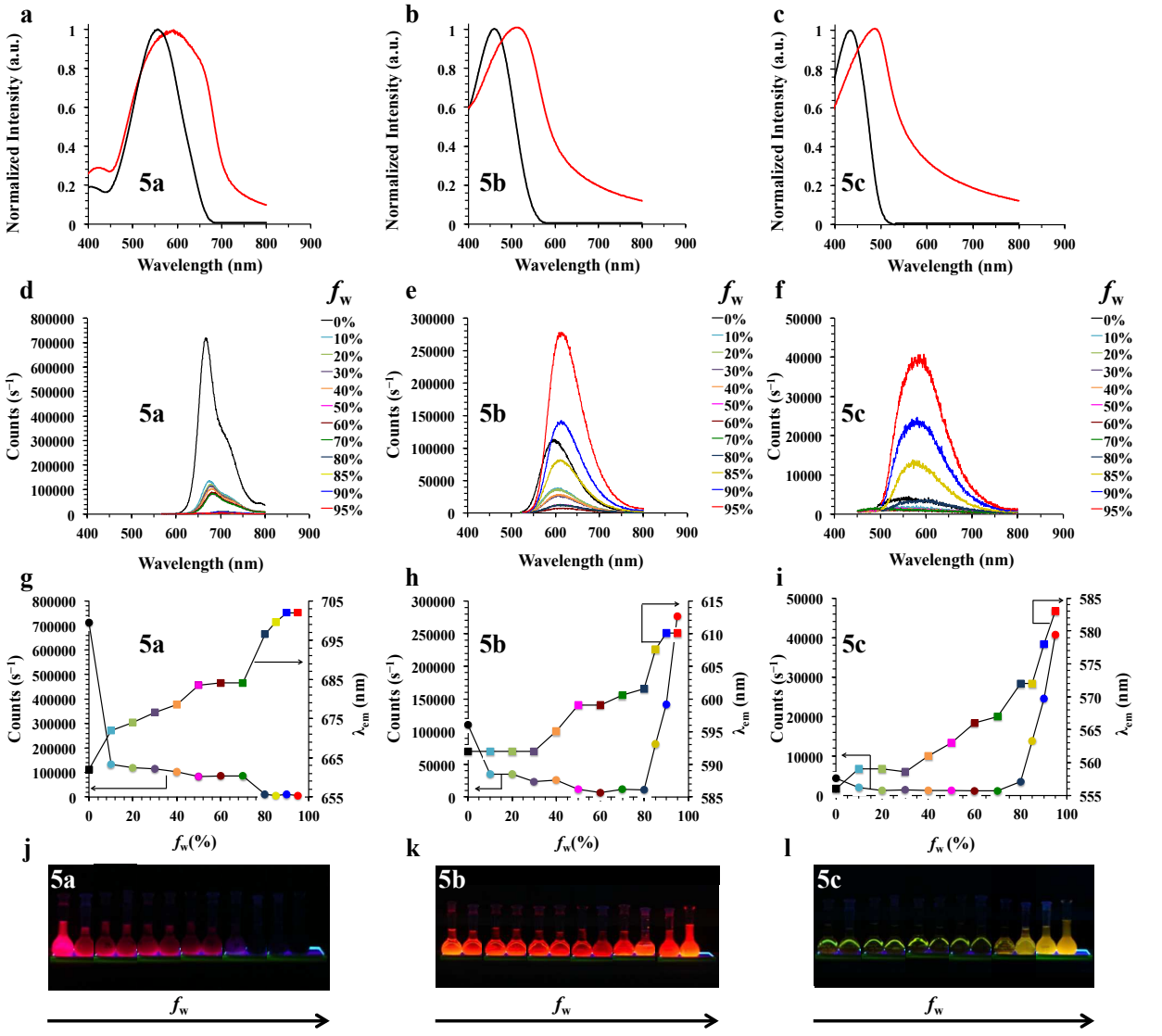

Fig. 1 Normalized UV-vis absorption spectra of **5a** (a), **5b** (b), and **5c** (c) in pure THF solution (black line) and in a THF-water mixture with water volume fraction (f_w) of 95% (red line) ([**5a–c**] = 250 µM). UV-vis emission spectra of **5a** (d), **5b** (e), and **5c** (f) in THF-water mixtures with f_w between 0% and 95% ([**5a–c**] = 250 µM). Changes in wavelength of maximum emission (λ_{em}) (squares) and emission intensity (circles) of **5a** (g), **5b** (h), and **5c** (i) in THF-water mixtures with f_w between 0% and 95% ([**5a–c**] = 250 µM). Visual representation of the aggregation-caused quenching observed for **5a** (j) and the aggregation-induced emission enhancement observed for **5b** and **5c** (k,l).

methoxyphenyl (**5b**: 62.0°, 60.5°) to 2,6-dimethoxyphenyl (**5c**: 74.6°, 66.6°). These data indicate that **5a** is more planar and therefore more electronically conjugated than **5b** and **5c** due to the absence of *ortho* methoxy substituents at the *N*-aryl rings on the 3-cyanoformazanate scaffold.

The electrochemical properties of **5c** were explored using cyclic voltammetry (Fig. S7 and Table S1). The complex exhibited two reversible one-electron reductions within the electrochemical window of acetonitrile ($E°_{red1}$ = −0.90 V, $E°_{red2}$ = −2.09 V relative to the ferrocene/ferrocenium redox couple). The results were compared to data obtained for **5a** ($E°_{red1}$ = −0.68 V, $E°_{red2}$ = −1.82 V) and **5b** ($E°_{red1}$ = −0.75 V, $E°_{red2}$ = −1.92 V) and demonstrated that the introduction of *ortho* methoxy substituents made electrochemical reduction more difficult due to a less planar π system.[16, 22]

Exploration of the AIEE behaviour of **5a−c** in THF-water mixtures with different volume fractions of water (f_w) revealed an interesting trend (Fig. 1 and Table S1). **5a** is a typical organic fluorophore, which undergoes detrimental ACQ accompanied by a red-shift in both the absorbance and emission maxima of 36 nm and 40 nm, respectively (Fig. 1 and Table S1). A plausible explanation for the ACQ effect is the presence of intermolecular π-electron interactions that are facilitated by the planar orientation of the *N*-aryl substituents. This hypothesis is corroborated by the solid-state structure of **5a**, which reveals short contacts (2.987−3.286 Å) between the formazanate backbone and the cyano substituent of a neighbouring molecule (Fig. 2a). The frontier molecular orbitals of **5a** have been shown previously to include significant orbital density on these structural features.[16] In addition, there are numerous intermolecular interactions [CH•••π (2.763 Å and 2.906 Å), CH•••O (2.707 Å and 3.060 Å), and CH•••F (2.478−2.665 Å)], which may enable the formation of excimers (Fig. S8).

Both **5b** and **5c** act as AIEgens and undergo AIEE likely as a result of RIM (Fig. 1 and Table S1). Initially (f_w = 0%), **5c** was weakly emissive and its emission intensity was further attenuated and red-shifted upon increasing f_w. The decrease in emission intensity as the solvent mixture became increasingly polar was consistent with previously observed behaviour for similar dyes.[16, 22] Upon reaching a critical f_w (70%), the emission intensity was revitalized and further intensified until it reached a maximum value at f_w = 95%. Interestingly, λ_{abs} and λ_{em} experience a net red-shift of 59 nm and 24 nm at f_w = 95% compared to f_w = 0% (Fig. 1 and Table S1). Based on the solid-state structure of **5c**, it is evident that there are multiple intermolecular interactions present: CH•••π (2.696 Å and 2.885 Å), CH•••O (3.113 Å and 3.125 Å), CH•••N (2.552 Å and 2.725 Å), and CH•••F (2.611 Å) (Fig. S9). These interactions lock the conformation of the *N*-aryl substituents and prevent intramolecular motion. Complex **5b** also exhibited decreased emission intensity upon the initial addition of water, which was rejuvenated at f_w = 80%. **5b** exhibited red-shifts of 61 nm (λ_{abs}) and 20 nm (λ_{em}) from f_w = 0% to f_w = 95% (Fig. 1 and Table S1) due to intermolecular interactions: CH•••π (2.655 Å and 2.788 Å), CH•••O (2.620 Å and 2.794 Å), and CH•••F (2.398 Å−2.509 Å) (Fig. S10). Red-shifted emission maxima are commonly observed for AIE-active molecules.[24] While we are unable to identify the specific interactions leading to the red-shift of the emission maxima observed for **5b** and **5c** (Figs. 2, S8−S10), we note that the potential π-stacking interactions observed in the solid-state structures of **5b** and **5c** have intermolecular distances outside the sum of the Van der Waal radii of the respective atoms (**5b**: 3.849−3.862 Å; **5c**: 3.747−3.758 Å).

In summary, the readily accessible BF_2 formazanates **5a−c** absorb and emit within the visible region of the electromagnetic spectrum. **5a** is a typical organic fluorophore that experienced ACQ whereas **5b** and **5c** exhibited AIEE. Controlled addition of water into THF solutions of **5b** and **5c** initially resulted in decreased emission intensity before a critical f_w (**5b**: 80%; **5c**: 70%) was reached and the emission intensity was invigorated

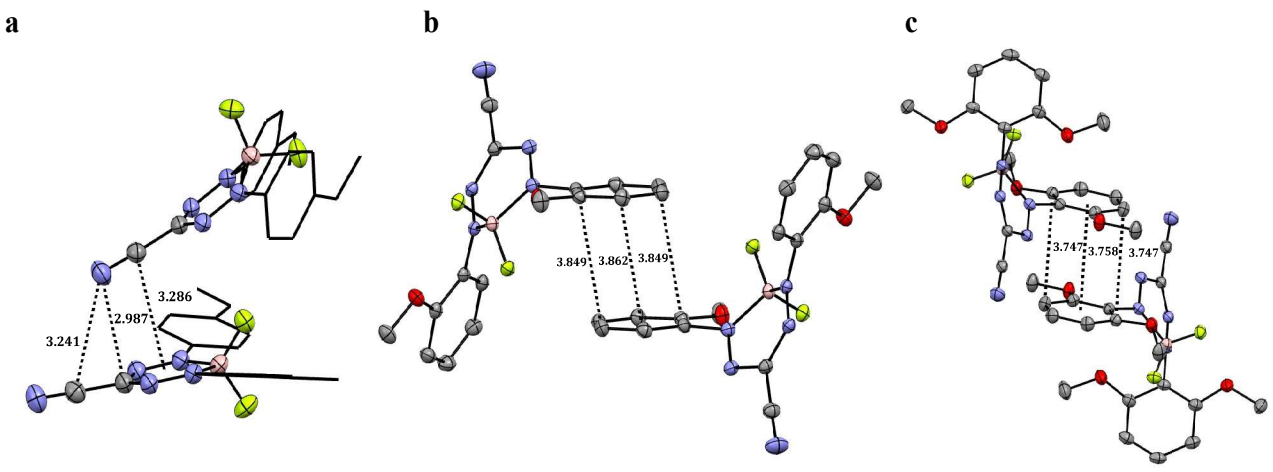

Fig. 2 Solid-state structures for **5a−c**. Intermolecular NC•••π [3.286 Å] and CN•••C [2.987 Å and 3.241 Å] interactions for **5a** (a).[16] Ring-slipped π-stacking motifs for **5b** (b),[22] and **5c** (c). Anisotropic displacement ellipsoids are shown at 50% probability. Hydrogen atoms have been omitted and *N*-aryl substituents in (a) have been converted to wireframe style for clarity. All distances are quoted in Å.

and enhanced. Complex **5b** exhibited a 3-fold increase in emission at f_w = 95%, while **5c** exhibited a 10-fold increase under the same conditions. The degrees of enhancement were significant, but less dramatic than those observed for CF_3- and COOMe-substituted boron dipyrromethenes (*ca.* 40-fold increase in glycerol/methanol), which emit at similar wavelengths.[25] The solid-state structure of **5a** indicated the presence of strong intermolecular π-interactions, which resulted in ACQ, while **5b** and **5c** exhibited AIEE due to the restriction of intramolecular motion upon aggregation and do not appear to π stack in the solid state.[26] This work highlights the potential of BF_2 formazanates as AIEgens. Subsequent studies will aim to further explore how substituent variation affects AIEE.

We would like to thank the University of Western Ontario, the Natural Science and Engineering Research Council (NSERC) of Canada (J.B.G.: DG, 435675 and R.R.M.: CGS-M Program), the Ontario Ministry of Research and Innovation (J.B.G.: ERA, ER14-10-147), and the Canadian Foundation for Innovation (J.B.G.: JELF, 33977) for funding this work. Finally, we thank Profs. E.R. Gillies and M.S. Workentin for access to instrumentation within their laboratories and Ms. S.M. Barbon for performing X-ray crystallography studies.

Notes and references

‡Two crystallographically independent molecules were observed within the unit cell previously determined for **5a**.[16]

1. a) J. Mei, N. L. C. Leung, R. T. K. Kwok, J. W. Y. Lam and B. Z. Tang, *Chem. Rev.*, 2015, **115**, 11718–11940; b) H. Wang, E. Zhao, J. W. Y. Lam and B. Z. Tang, *Mater. Today*, 2015, **18**, 365–377.
2. a) W. Z. Yuan, Y. Gong, S. Chen, X. Y. Shen, J. W. Y. Lam, P. Lu, Y. Lu, Z. Wang, R. Hu, N. Xie, H. S. Kwok, Y. Zhang, J. Z. Sun and B. Z. Tang, *Chem. Mater.*, 2012, **24**, 1518–1528; b) J. Yang, J. Huang, N. Sun, Q. Peng, Q. Li, D. Ma and Z. Li, *Chem. Eur. J.*, 2015, **21**, 6862–6868; c) B. Liu, H. Nie, X. Zhou, S. Hu, D. Luo, D. Gao, J. Zou, M. Xu, L. Wang, Z. Zhao, A. Qin, J. Peng, H. Ning, Y. Cao and B. Z. Tang, *Adv. Funct. Mater.*, 2016, **26**, 776–783.
3. R. T. K. Kwok, C. W. T. Leung, J. W. Y. Lam and B. Z. Tang, *Chem. Soc. Rev.*, 2015, **44**, 4228–4238.
4. a) M. Wang, G. Zhang, D. Zhang, D. Zhu and B. Z. Tang, *J. Mater. Chem.*, 2010, **20**, 1858–1867; b) X. Dong, F. Hu, Z. Liu, G. Zhang and D. Zhang, *Chem. Commun.*, 2015, **51**, 3892–3895; c) G. Feng, Y. Yuan, H. Fang, R. Zhang, B. Xing, G. Zhang, D. Zhang and B. Liu, *Chem. Commun.*, 2015, **51**, 12490–12493.
5. J. Mei, Y. Hong, J. W. Y. Lam, A. Qin, Y. Tang and B. Z. Tang, *Adv. Mater.*, 2014, **26**, 5429–5479.
6. a) H. Shi, R. T. K. Kwok, J. Liu, B. Xing, B. Z. Tang and B. Liu, *J. Am. Chem. Soc.*, 2012, **134**, 17972–17981; b) Y. Li, Y. Wu, J. Chang, M. Chen, R. Liu and F. Li, *Chem. Commun.*, 2013, **49**, 11335–11337.
7. J. B. Birks, *Photophysics of Aromatic Molecules*, Wiley, New York, 1970.
8. J. Luo, Z. Xie, J. W. Y. Lam, L. Cheng, H. Chen, C. Qiu, H. S. Kwok, X. Zhan, Y. Liu, D. Zhu and B. Z. Tang, *Chem. Commun.*, 2001, 1740–1741.
9. a) J. W. Levell, A. Ruseckas, J. B. Henry, Y. Wang, A. D. Stretton, A. R. Mount, T. H. Galow and I. D. W. Samuel, *J. Phys. Chem. A*, 2010, **114**, 13291–13295; b) Z. He, L. Shan, J. Mei, H. Wang, J. W. Y. Lam, H. H. Y. Sung, I. D. Williams, X. Gu, Q. Miao and B. Z. Tang, *Chem. Sci.*, 2015, **6**, 3538–3543;
c) Z. He, L. Zhang, J. Mei, T. Zhang, J. W. Y. Lam, Z. Shuai, Y. Q. Dong and B. Z. Tang, *Chem. Mater.*, 2015, **27**, 6601–6607.
10. a) B.-K. An, S.-K. Kwon, S.-D. Jung and S. Y. Park, *J. Am. Chem. Soc.*, 2002, **124**, 14410–14415; b) T. L. Bandrowsky, J. B. Carroll and J. Braddock-Wilking, *Organometallics*, 2011, **30**, 3559–3569; c) Y. Ren and T. Baumgartner, *Inorg. Chem.*, 2012, **51**, 2669–2678; d) G. He, W. Torres Delgado, D. J. Schatz, C. Merten, A. Mohammadpour, L. Mayr, M. J. Ferguson, R. McDonald, A. Brown, K. Shankar and E. Rivard, *Angew. Chem. Int. Ed.*, 2014, **53**, 4587–4591.
11. a) Y. Yang, X. Su, C. N. Carroll and I. Aprahamian, *Chem. Sci.*, 2012, **3**, 610–613; b) R. Yoshii, A. Hirose, K. Tanaka and Y. Chujo, *Chem. Eur. J.*, 2014, **20**, 8320–8324; c) H. Naito, Y. Morisaki and Y. Chujo, *Angew. Chem. Int. Ed.*, 2015, **54**, 5084–5087; d) T. Butler, W. A. Morris, J. Samonina-Kosicka and C. L. Fraser, *ACS Appl. Mater. Interfaces*, 2016, **8**, 1242–1251; e) D. Wu, L. Shao, Y. Li, Q. Hu, F. Huang, G. Yu and G. Tang, *Chem. Commun.*, 2016, **52**, 541–544.
12. a) R. Hu, C. F. A. Gómez-Durán, J. W. Y. Lam, J. L. Belmonte-Vázquez, C. Deng, S. Chen, R. Ye, E. Peña-Cabrera, Y. Zhong, K. S. Wong and B. Z. Tang, *Chem. Commun.*, 2012, **48**, 10099–10101; b) T. T. Vu, M. Dvorko, E. Y. Schmidt, J.-F. Audibert, P. Retailleau, B. A. Trofimov, R. B. Pansu, G. Clavier and R. Méallet-Renault, *J. Phys. Chem. C.*, 2013, **117**, 5373–5385; c) S. Mukherjee and P. Thilagar, *Chem. Eur. J.*, 2014, **20**, 9052–9062; d) C. F. A. Gómez-Durán, R. Hu, G. Feng, T. Li, F. Bu, M. Arseneault, B. Liu, E. Peña-Cabrera and B. Z. Tang, *ACS Appl. Mater. Interfaces*, 2015, **7**, 15168–15176.
13. Z. Zhao, J. W. Y. Lam and B. Z. Tang, *J. Mater. Chem.*, 2012, **22**, 23726–23740.
14. a) N. B. Shustova, B. D. McCarthy and M. Dincă, *J. Am. Chem. Soc.*, 2011, **133**, 20126–20129; b) X. Yan, H. Wang, C. E. Hauke, T. R. Cook, M. Wang, M. L. Saha, Z. Zhou, M. Zhang, X. Li, F. Huang and P. J. Stang, *J. Am. Chem. Soc.*, 2015, **137**, 15276–15286.
15. a) M. Yang, D. Xu, W. Xi, L. Wang, J. Zheng, J. Huang, J. Zhang, H. Zhou, J. Wu and Y. Tian, *J. Org. Chem.*, 2013, **78**, 10344–10359; b) M. Chen, H. Nie, B. Song, L. Li, J. Z. Sun, A. Qin and B. Z. Tang, *J. Mater. Chem. C.*, 2016, **4**, 2901–2908.
16. S. M. Barbon, P. A. Reinkeluers, J. T. Price, V. N. Staroverov and J. B. Gilroy, *Chem. Eur. J.*, 2014, **20**, 11340–11344.
17. a) A. W. Nineham, *Chem. Rev.*, 1955, **55**, 355–483; b) A. S. Shawali and N. A. Samy, *J. Adv. Res.*, 2015, **6**, 241–254.
18. M. V. Berridge, P. M. Herst and A. S. Tan, *Tetrazolium dyes as tools in cell biology: New insights into their cellular reduction*, Elsevier, 2005.
19. a) S. Novoa, J. A. Paquette, S. M. Barbon, R. R. Maar and J. B. Gilroy, *J. Mater. Chem. C.*, 2016, **4**, 3987–3994; b) S. M. Barbon and J. B. Gilroy, *Polym. Chem.*, 2016, **7**, 3589–3598.
20. M. Hesari, S. M. Barbon, V. N. Staroverov, Z. Ding and J. B. Gilroy, *Chem. Commun.*, 2015, **51**, 3766–3769.
21. M.-C. Chang and E. Otten, *Inorg. Chem.*, 2015, **54**, 8656–8664.
22. R. R. Maar, S. M. Barbon, N. Sharma, H. Groom, L. G. Luyt and J. B. Gilroy, *Chem. Eur. J.*, 2015, **21**, 15589–15599.
23. Attempts to determine the absolute fluorescence quantum yields for the aggregate solutions and thin films using the integrating sphere method were unsuccessful due to significant photon reabsorption by the samples.
24. a) R. Hu, E. Lager, A. Aguilar-Aguilar, J. Liu, J. W. Y. Lam, H. H. Y. Sung, I. D. Williams, Y. Zhong, K. S. Wong, E. Peña-Cabrera and B. Z. Tang, *J. Phys. Chem. C.*, 2009, **113**, 15845–15853; b) Q. Dai, W. Liu, L. Zeng, C.-S. Lee, J. Wu and P. Wang, *CrystEngComm*, 2011, **13**, 4617–4624; c) C.-W. Liao, R. Rao M. and S.-S. Sun, *Chem. Commun.*, 2015, **51**, 2656–2659; d) R. S. Singh, R. K. Gupta, R. P. Paitandi, M. Dubey, G. Sharma, B. Koch and D. S. Pandey, *Chem. Commun.*, 2015, **51**, 9125–9128.
25. a) S. Choi, J. Bouffard and Y. Kim, *Chem. Sci.*, 2014, **5**, 751–755; b) S. Kim, J. Bouffard and Y. Kim, *Chem. Eur. J.*, 2015, **21**, 17459–17465.
26. The thin-film absorption and emission spectra for **5b** and **5c** overlap significantly. However, the films appear to be highly luminescent under UV irradiation (Fig. S11). Complex 5a is non-emissive in the solid state.

Graphical Abstract

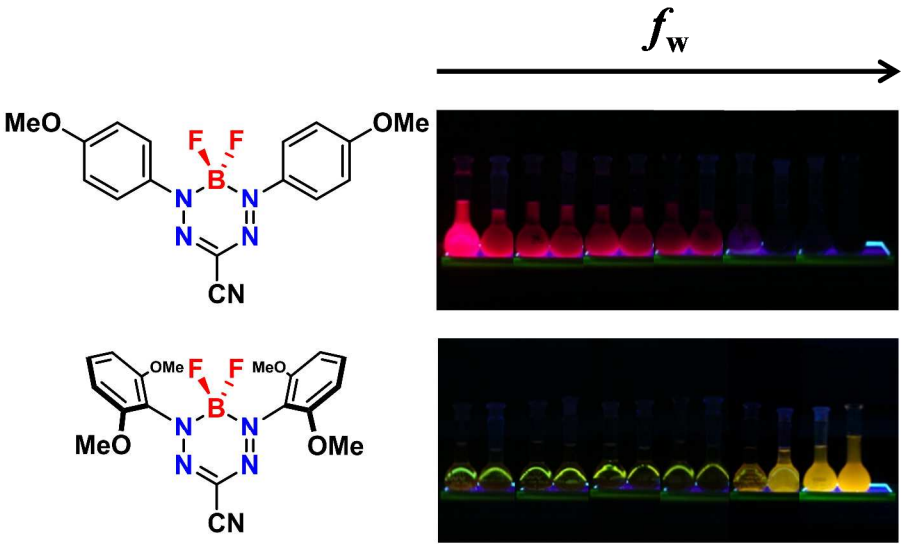

Boron difluoride (BF_2) complexes of 3-cyanoformazanates exhibit aggregation-induced emission enhancement in THF-water mixtures due to their severely twisted *N*-aryl substituents which restrict intramolecular motion and π stacking upon aggregation.